Use of zero-frequency resonator for automatically detecting systolic peaks of photoplethysmogram signal

Simhadri Vadrevu ✉, *M. Sabarimalai Manikandan*

School of Electrical Sciences, Indian Institute of Technology Bhubaneswar, Kurdha, Odisha-752050, India
✉ *E-mail: vs12@iitbbs.ac.in*

Published in Healthcare Technology Letters; Received on 19th May 2018; Revised on 16th February 2019; Accepted on 26th February 2019

This work investigates the application of zero-frequency resonator (ZFR) for detecting systolic peaks of photoplethysmogram (PPG) signals. Based on the authors' studies, they propose an automated noise-robust method, which consists of the central difference operation, the ZFR, the mean subtraction and averaging, the peak determination, and the peak rejection/acceptance rule. The method is evaluated using different kinds of PPG signals taken from the standard MIT-BIH polysomnographic database and Complex Systems Laboratory database and the recorded PPG signals at their Biomedical System Lab. The method achieves an average sensitivity (Se) of 99.95%, positive predictivity (Pp) of 99.89%, and overall accuracy (OA) of 99.84% on a total number of 116,673 true peaks. Evaluation results further demonstrate the robustness of the ZFR-based method for noisy PPG signals with a signal-to-noise ratio (SNR) ranging from 30 to 5 dB. The method achieves an average Se = 99.76%, Pp = 99.84%, and OA = 99.60% for noisy PPG signals with a SNR of 5 dB. Various results show that the method yields better detection rates for both noise-free and noisy PPG signals. The method is simple and reliable as compared with the complexity of signal processing techniques and detection performance of the existing detection methods.

1. Introduction: The photoplethysmography (PPG) is a simple, inexpensive and non-invasive optical technique for recording and monitoring blood volume in tissue as a function of time [1–7]. The PPG signal is used in many clinical applications such as cardiovascular monitoring, vascular assessment, and autonomic function assessment. The PPG waveform may consist of five distinct characteristic points such as the pulse onset, the systolic peak (or the percussion peak), the tidal wave, the dicrotic notch (or the incisura wave), and the dicrotic wave peak [5–7]. The pulse onset represents minimum blood volume changes, which indicates the beginning of ventricular contraction and ejection of blood into the aorta (early systole). The systolic peak represents the maximum blood volume changes, which indicates the end of blood ejection. The tidal wave is the peak of the pulse wave in the later systole. The dicrotic notch represents the closure of the aortic valve, i.e. the beginning of the diastole phase. Despite the different kinds of normal and pathological PPG signals, the systolic peak instant, which is more prominent in the PPG signal, is most widely used for measurement of diagnostic markers such as pulse rate (PR), respiration rate, pulse transit time, cuff-less blood pressure and arterial stiffness. Furthermore, the pulse peak instants are used as reference points for determining other characteristic points of the pulse signal, heart sound (S1/S2) identification, PPG biometric template extraction, and emotion recognition. Therefore, automatic detection of the systolic peak has become one of the essential preprocessing steps in most automated PPG signal analysis applications.

1.1. Existing methods: Many methods were presented based on different signal processing techniques [5–16]. Most methods include three major stages: (i) preprocessing stage for removal of background noises; (ii) candidate feature (or envelope waveform) extraction stage; and (iii) peak finding stage. In [4], three detection methods were proposed: (i) symmetrical curve fitting method; (ii) Gaussian curve fitting method; and (iii) adaptive curve fitting method to reveal the secondary peak of the PPG signal. Jang *et al.* [9] presented a method which uses the digital filter for removal of baseline wanders. The cut-off frequency of 0.5 Hz was based on the PR <40 bpm (0.67 Hz) is practically uncommon and human respiration, and also the main components of baseline wander occur within the bandwidth of 0.15–0.5 Hz. Then, a slope sum function (SSF) was presented to enhance an up-slope of the digital volume pulse (DVP) signal and to suppress its down-slope. The pulse peaks were identified based on the analysis of the slope, amplitude, and width. In [7], the fourth-order Chebyshev type I bandpass filter was designed with a bandwidth of 0.5–16 Hz to remove the noise and baseline distortion in the PPG signals. The Shannon energy envelope was extracted from the normalised filtered PPG signal. The onset and peak-finding were implemented based on the Hilbert transformation, drift removal, zero-crossing point detection, and minimum value detection. In [8], the bandpass filter with a cut-off frequency ranging from 0.5 to 5.5 Hz was used for removal of background noises. The pulse wave maxima were extracted with slope criteria for fining the peaks and onsets. In [9], a modified morphological filter was employed for removing baseline wanders. The SSF with an adaptive thresholding scheme is used for detecting the pulse peaks from a baseline-removed DVP signal. In [10], knowledge-based rules using the estimated parameters such as pulse duration, height, area, and previous pulse onsets for detecting the pulse peaks. In [11], an adaptive threshold approach was proposed using the directional threshold with a fixed slope parameter, which is updated based on past peak information. In [12], a template matching approach was proposed using the cross-correlation coefficients with a three-point peak detection algorithm. The detection rate of this approach highly relies on the selection of a noise-free reference template waveform under noisy PPG recording conditions. In [13], a multi-stage mixed detection approach is presented based on the zero-crossing and local minima and maxima. In [14], a linear-phase finite impulse response low-pass-differentiator filter with a transition band between 7.7 and 8 Hz was employed to emphasise the abrupt slopes of the PPG signal. In [15], a PPG waveform delineation method was proposed using derivative and zero crossing schemes on the derivative envelope. In [16], the singular value decomposition and smoothing using a moving average filter were used for suppression of baseline wanders and extraction of the most periodic components. The peak and onset points were found by finding local maxima and minima on the selected intrinsic mode functions (IMFs). The spectral information of noise and PPG signal may be distributed over different IMFs

under different kinds of pulse and noise patterns. Thus, it is difficult to automate the process of selection of IMFs for constructing the candidate PPG signal and suppression of different kinds of noises and artefacts. In [17], an ensemble empirical mode decomposition (EMD)-based algorithm was proposed that integrates real-time atrial blood pressure (ABP) delineation and quality assessment. The ensemble empirical mode decomposition (EEMD) frequency selectivity is used for both delineation and artefact detection. In [18], an automatic method was proposed based on the Gaussian derivative filtering, non-linear peak amplification, Gaussian derivative-based peak finding scheme, and peak position adjustment procedure. In [17], the EMD detrending algorithm was presented to remove noise and artefacts in the PPG signal. Some of the past studies showed that EMD is a computationally expensive algorithm. The failure case of the find peak function of the MATLAB is demonstrated in Fig. 1 for the PPG signal with varying pulse amplitudes.

Literature survey shows that most methods employed the search-back algorithm with sets of decision rules in order to eliminate over-detected pulse peaks and to re-estimate missed ones under high-frequency noises and artefacts. These decision rules are based on the assumption that a difference between two adjacent pulses cannot be beyond certain range as the pulse is a slowly time-varying signal. This assumption may not be satisfied in practice due to the sudden variations in the irregular pulse rates even within the pulse rates of a human subject. Although the peak detection is relatively accurate in the case of noise-free PPG signals, an accurate and reliable determination of systolic peaks is a still challenging task in the presence of different kinds of pulse patterns, irregular pulse rates, sudden change in pulse peak amplitudes and pulse rates, low-amplitude pulses and various kinds of noise sources.

1.2. Key contribution and organisation of the Letter: In this Letter, we investigate the application of zero-frequency resonator (ZFR) for automatically determining the systolic peaks of the PPG signal. Based on our studies, this Letter proposes an automated noise-robust method by combining the smoothing processing and peak acceptance/rejection rule with the ZFR. The remainder of the Letter is organised as follows. Section 2 presents the stages of the ZFR-based method. Section 3 presents evaluation results and performance comparison with other existing methods for the same signal databases. Finally, conclusions are drawn in Section 4.

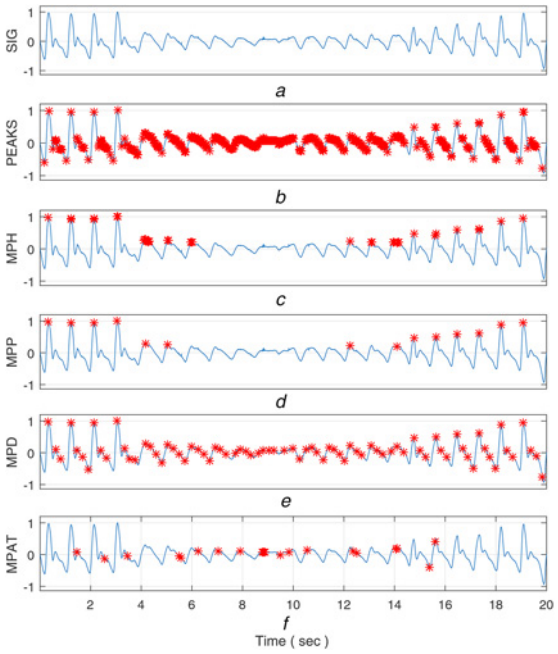

Fig. 1 *Illustrates the failure case of the find peak function of the MATLAB for the PPG signal with varying amplitudes*
a Original signal from MIT-BIH SLP: 'slp41m'
b Peaks detected without post-processing
c Peaks detected using find peak function with minimum peak height
d Peaks detected using find peak function with minimum peak prominence
e Peaks detected using find peak function with minimum peak distance
f Peaks detected using find peak function with minimum peak threshold

2. Materials and methods:

2.1. Overview of ZFR: The use of ZFR was demonstrated in the task of detection of glottal closure instants (GCIs) [19]. The ZFR whose central frequency located at 0 Hz can have the information of the discontinuities. We also studied the robustness of the ZFR for detection of GCIs from the electroglottography signal [20]. The output of ZFR is an exponentially growing/decaying signal. The trend of the signal is removed to extract the relevant information. In this work, we study the robustness of the ZFR for detecting the systolic peaks of the PPG signal. The trend removed signal mainly exhibits the slope portion of the PPG signal. Unlike other methods, the ZFR-based candidate waveform extraction approach is much simpler because it includes difference operation, ZFR, and mean subtraction. A block diagram of the proposed automated systolic peak detection method is shown in Fig. 2, which consists of the following major steps:

2.2. Noise suppression: In the first step, removal of the dc or low frequency baseline wanders from a PPG signal $x[n]$ is performed using a central differencing, which is implemented as

$$d[n] = x[n+1] - x[n-1]. \tag{1}$$

The output of this step is shown in Fig. 3*a2* for the PPG signals recorded using different kinds of sensors. The main objective of the application of central difference operation is to reduce the amplitude of the high-frequency noise components and remove the low-frequency baseline components.

2.3. Zero-Frequency resonator: In the second step, the differenced signal $d[n]$ is passed twice through a ZFR [19], which is implemented as

$$y_1[n] = -\sum_{k=1}^{2} a_k y_1[n-k] + x[n], \tag{2}$$

$$y_2[n] = -\sum_{k=1}^{2} a_k y_2[n-k] + y_1[n], \tag{3}$$

where $a_1 = -2$ and $a_2 = 1$. The output of the ZFR step is shown in Fig. 3*a3*. It has been noted that the ZFR is an exponentially growing/decaying signal, $y_2[n]$.

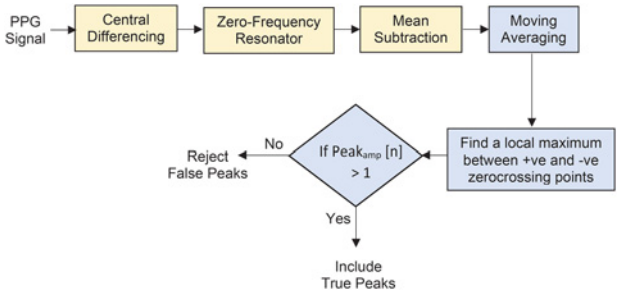

Fig. 2 *Block diagram of the ZFR-based systolic peak detection method*

doi: 10.1049/htl.2018.5026

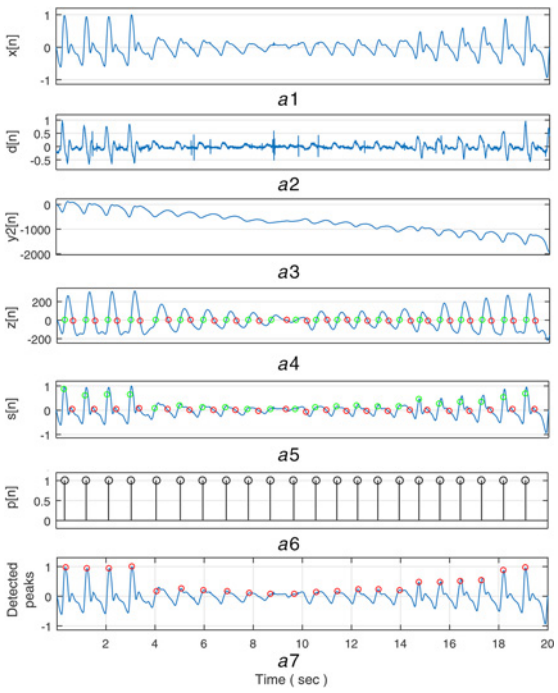

Fig. 3 *Results of each of the steps of the ZFR-based peak detection method*
a1 Original PPG signal
a2 Central differencing
a3 ZFR
a4 Mean subtraction
a5 Moving averaging
a6 Peak determination
a7 Detected peaks

2.4. Mean subtraction: In the third step, the trend in the ZFR output $y_2[n]$ is removed by subtracting the mean of the short-term window of the signal $y_2[n]$. In this study, a window with a duration of 1000 ms at each sample location is fixed to remove the trend from a signal $y_2[n]$. The resulting mean subtracted signal is called the zero frequency filtered signal (ZFFS) [19], which is implemented as

$$z[n] = y_2[n] - \frac{1}{2N+1}\sum_{m=-N}^{N} y_2[n+m], \tag{4}$$

where the window size is chosen based on the pulse interval range. The output of the mean subtraction step is shown in Fig. 3*a4*. Results show that the ZFFS is the oscillating waveform with local periods approximately equal to the local pulse periods. From the preliminary studies, it has been noted the presence of spurious spikes, which may lead to more false positives under high-level high-frequency noises. Furthermore, the presence of the multiple and/or unsymmetrical local peaks (around the systolic peak portion) in the ZFFS signal $z[n]$ can lead to an inaccurate measurement of time instants of the systolic peaks. Therefore, the smoothing of the ZFFS is performed in this study.

2.5. Moving averaging: In the fourth step, in order to reduce the effects of spurious noise spikes and multiple peaks, a moving average is applied with a window of 200 ms to obtain the smoothed peak signal. The moving average is implemented as

$$s[k] = \frac{1}{2K+1}\sum_{k=-K/2}^{K/2} z[k], \tag{5}$$

where K denotes the window size. The output of the moving average is shown in Fig. 3*a5*. From the results, it has been noticed that the presence of a true systolic peak is in between the positive and negative zero-crossing points of the smoothed ZFFS signal $s[n]$. Therefore, the zero-crossing points are detected and used as guides in determining the true systolic peaks in the PPG signal.

2.6. Peak determination: In the fifth step, the systolic peak of the PPG signal is determined by finding the maximum of a windowed PPG segment extracted within the locations of positive zero-crossing point and negative zero-crossing point of the ZFFS signal. The time instants of the detected peaks are shown in Figs. 3–5. From the detection results, it is noted that the method produces more false positives for the PPG signals with long pauses between two consecutive systolic peaks, as shown in Fig. 5. Therefore, the peak-amplitudes between the zero-crossing points are compared with a predefined threshold.

2.7. Peak acceptance/rejection rule: From our preliminary studies, it is noted that the ZFFS signal has the minimum peak amplitude ranging from −5 to 5 for a wide variety of PPG signals including low-amplitude systolic peaks, time-varying peak-amplitudes and wave shapes, different slope variations (from pulse onset to peak) and other local waves such as the tidal wave, the dicrotic notch, and the dicrotic wave. Thus, a predefined peak-amplitude threshold of 1 is chosen to accept/reject a detected peak. If the peak-amplitude is >1 then the detected peak is considered as a true positive otherwise it is considered as a noise peak which can be discarded in the detection process.

3. Results and discussion: The accuracy and robustness of the ZFR-based systolic peak detection method is validated using a large scale of PPG signals taken from the standard such as MIT-BIH polysomnographic database (SLP) (http://www.physionet.org/physiobank/database/slpdb/) [21] and Complex Systems Laboratory (CSL) database [22] and the recorded PPG signals in our Biomedical System Lab.

3.1. Experimental set-up: In this study, we created the PPG signal databases using the commercially available PPG acquisition hardware modules such as Pulse Oximeter TMS320C5515 Medical Development Kit [23], and our finger pulse sensing module. The TI pulse oximeter system monitors the oxygen saturation of a patient's blood non-invasively. The magnitude of the PPG signal depends on the amount of blood ejected from the heart during the systolic cycle, the optical absorption of blood, the absorption by the skin and various tissue components, and the specific wavelengths used to illuminate the vascular tissue bed [23]. The fully integrated TI analogue front sensing module end consists of trans-impedance amplifier gain, ambient light compensation, additional stage 2 gain, and light-emitting diode (LED) current, an analogue-to-digital converter, an LED transmit section, diagnostics for sensor and LED fault detection, a sensing probe, a wireless module and an ultra-low power microcontroller for calculating an oxygen saturation (SpO2) level. The PPG signals are collected from 20 subjects for performance validation purpose. The acquired PPG signals are resampled to a sampling rate of 125 Hz. The PPG signals are often corrupted with different kinds of motion artefacts, power-line interference, and other high-frequency noises.

3.2. Description of the PPG databases: The MIT-BIH SLP database is a collection of recordings of multiple physiologic signals during sleep [21]. The SLP database was created for the evaluation of chronic obstructive sleep apnea syndrome and the effects of medical intervention. The PPG records 'slp01a' and 'slp01b' are segments of one subject's polysomnogram, separated by a gap of about 1 h. The PPG records 'slp02a' and 'slp02b' are segments of another subject's polysomnogram, separated by a 10-min gap. The remaining 14 records are from different subjects [21]. The

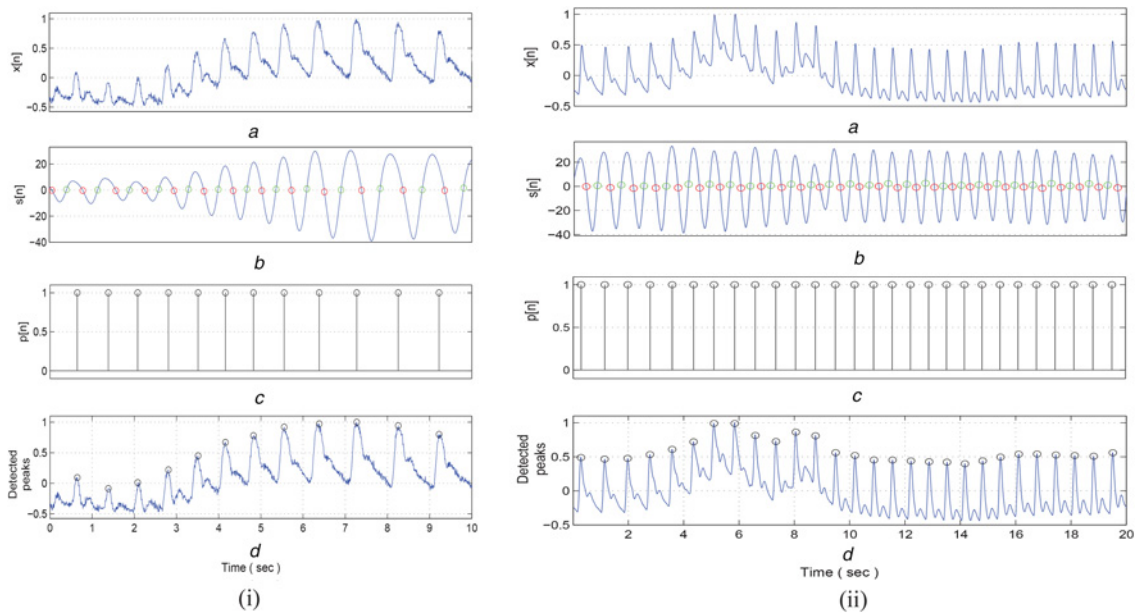

Fig. 4 *Performance of the proposed method*
a Original PPG
b ZFFS signal
c Detected candidate peak location
d Detected systolic peaks for (**i**) the PPG signal with time-varying systolic peak amplitudes, the baseline wander and high-frequency noises; and (**ii**) the PPG signal with varying pulse shapes and baseline wander

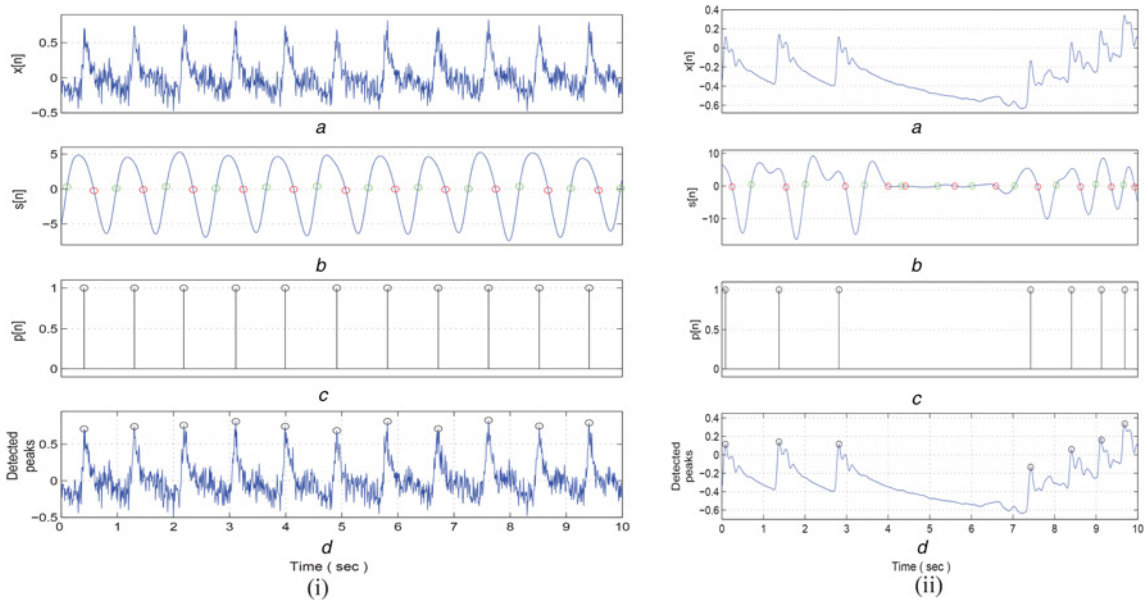

Fig. 5 *Performance of the proposed method*
a Original PPG
b ZFFS signal
c Detected candidate peak location
d Detected systolic peaks for (i) the noisy PPG signal with corrupted AWGN, with SNR = 5 dB; and (**ii**) the PPG signal with baseline wander and long pause. It is noted that the ZFR-based method results in some peaks for the long pause portion but the proposed peak acceptance/rejection rule improves the detection performance by discarding the detected peaks with peak-amplitudes which are <1

recordings were digitised at a sampling interval of 250 Hz and 12 bits/sample.

The CSL database contains 60 min manually annotated recordings from six patients that were acquired by a data acquisition system in the CSL [22]. The benchmark CSL database made it openly accessible for beat detector evaluation. The CSL database is most widely used to evaluate the performance of the systolic peak detection methods. The ABP signals were obtained from two paediatric cases in the paediatric intensive care unit. These signals were sampled at 125 Hz, band-pass filtered and auto-scaled. The CSL database contains manual beat annotations from two independent experts and the automatic annotation from the CSL Reference algorithm [5]. The annotations of the expert with identification 'DT' are chosen as reference beats in this study. The beat annotations are provided in the database. We manually annotated the systolic peak locations for our real-time PPG signals that are recorded using the Bioradio, TI Pulse oximeter, and other commercial available PPG sensing hardware. In addition with the noises

doi: 10.1049/htl.2018.5026

introduced to the PPG signals while recordings, the noisy PPG signals are also created by adding the simulated additive white Gaussian noise (AWGN), powerline interference and motion artefacts to the recorded PPG signals.

3.3. Performance metrics: In this study, detection results are evaluated using the standard benchmark metrics such as sensitivity (Se), positive predictivity (Pp), detection error rate (DER) and overall accuracy (OA) [15–18] that are computed as

$$\mathrm{Se} = \mathrm{TP}/(\mathrm{TP} + \mathrm{FN}) \times 100\%, \quad (6)$$

$$\mathrm{Pp} = \mathrm{TP}/(\mathrm{TP} + \mathrm{FP}) \times 100\%, \quad (7)$$

$$\mathrm{DER} = (\mathrm{FP} + \mathrm{FN})/\mathrm{TS} \times 100\%, \quad (8)$$

$$\mathrm{OA} = \mathrm{TP}/(\mathrm{TP} + \mathrm{FP} + \mathrm{FN}) \times 100\%, \quad (9)$$

where TP denotes the true positive when a systolic peak is correctly detected, FN denotes false negative when a systolic peak is not detected, FP denotes the false positive when a noise peak is detected as a systolic peak and TS denotes the total systolic peaks. These detection parameters are found by comparing the detected peak locations with the expert beat-beat annotations given in the PPG database. The detected systolic peaks are considered true positives if the peaks are within a predefined acceptance interval of 10 ms otherwise the detected peaks are considered as false positives.

3.4. Detection performance evaluation: The main objective of this study to investigate the accuracy and robustness of the ZFR-based method for detecting the systolic peaks of the PPG signal. The method is tested using a wide variety of PPG signals and different kinds of noises and artefacts. The detection performance of the method is summarised in Tables 1 and 2 for the MIT-BIH SLP database and IITBBS database. From the results of Table 1, it is noted that the method yields a Se of 99.95–100% for most test records except the record 'slp41m' and Pp of 99.85–100% for most records except the records: 'slp01bm', 'slp02am', 'slp02bm', and 'slp41m'. Based on the visual inspection of detection results, it is noted that these records have severe motion artefacts. The method has a FN of 13 peaks due to the presence of very small local PPG waves. Results show that the method has a DER of 127 peaks for a total of 87,342 peaks taken from the 18 PPG records of the MIT-BIH SLP database. The performance of the method is further evaluated using the real-time PPG signals that are recorded in the Biomedical System Laboratory at IIT Bhubaneswar. The detection results are summarised in Table 2 for 20 PPG signals taken from the IITBBS PPG databases. Results demonstrate that the method achieves a Se of 100% for most test PPG signals and a Pp of 100% except for six subjects. However, the method has an OA ranging from 99 to 100%. For a total of 16,244 peaks taken from the 20 subjects of the IITBBS PPG database, the method yields an average Se of 99.95%, Pp of 99.93% and OA of 99.88% for different kinds of PPG waveform patterns and noises. The detection results are shown in Figs. 3–5 for different kinds of PPG signals with irregular pulse rates, pulse shapes and long pause and also corrupted with baseline wanders and AWGNs.

3.5. Performance comparison: In this study, the detection rates of the method are compared with the existing methods on the MIT-SLP and CSL databases. Since the design parameters of the existing methods are not available for implementation purpose, the detection results of existing methods are considered for performance comparison. In this study, we have taken a total of 87,342 systolic peaks from the records of the MIT-BIH SLP database. Furthermore, the performance of the method is evaluated on a total of 13,079 systolic peaks of the CSL database. Evaluation results of the detection methods on both benchmark PPG databases are summarised in Table 3. Results show that the method yields better detection rates as compared with the existing methods and CSL Reference methodologies for both PPG signal databases [15, 17, 18]. Unlike other derivative-based methods, the ZFFS signal can be used as a better candidate waveform for determining the peaks in the PPG signal by detecting the zero-crossing points. The proposed method is straightforward in the sense that our method does not include any search-back algorithms for including or rejecting the missed or noise peaks.

3.6. Robustness evaluation: The robustness of the method is evaluated on the standard CSL databases by adding the synthetic AWGN. Table 4 summarises the detection rates of the method

Table 1 Peak detection performance on the MIT-BIH SLP database

Record	TP	FP	FN	DER, %	Se, %	Pp, %	OA, %
slp01am	4206	0	0	0	100	100	100
slp01bm	4195	42	1	1.03	99.98	99.01	99
slp02am	6021	10	4	0.23	99.93	99.83	99.77
slp02bm	5298	9	4	0.25	99.92	99.83	99.76
slp03m	4402	1	0	0.02	100	99.98	99.98
slp04m	5345	0	0	0	100	100	100
slp14m	4176	2	2	0.10	99.95	99.95	99.90
slp16m	5605	2	0	0.04	100	99.96	99.96
slp32m	4475	2	0	0.04	100	99.96	99.96
slp37m	5592	0	0	0	100	100	100
slp41m	4599	17	13	0.65	99.72	99.63	99.35
slp45m	5019	0	0	0	100	100	100
slp48m	4548	5	0	0.11	100	99.89	99.89
slp59m	4960	0	0	0	100	100	100
slp60m	4863	0	0	0	100	100	100
slp61m	4926	6	2	0.16	99.96	99.88	99.84
slp66m	4517	3	2	0.11	99.96	99.93	99.89
slp67xm	4567	0	0	0	100	100	100
overall	87,314	99	28	0.15	99.97	99.89	99.85

Table 2 Peak detection performance on the IITBBS database

Record	TP	FP	FN	DER, %	Se, %	Pp, %	OA, %
subj01	923	4	4	0.87	99.57	99.57	99.14
subj02	802	0	0	0	100	100	100
subj03	767	0	0	0	100	100	100
subj04	880	1	0	0.11	100	99.89	99.89
subj05	797	2	0	0.25	100	99.75	99.75
subj06	725	0	0	0	100	100	100
subj07	880	0	0	0	100	100	100
subj08	932	0	0	0	100	100	100
subj09	852	0	0	0	100	100	100
subj10	854	0	0	0	100	100	100
subj11	677	0	0	0	100	100	100
subj12	921	3	3	0.65	99.68	99.68	99.35
subj13	760	0	0	0	100	100	100
subj14	954	0	0	0	100	100	100
subj15	687	1	0	0.15	100	99.85	99.85
subj16	685	0	0	0	100	100	100
subj17	737	0	0	0	100	100	100
subj18	633	1	1	0.32	99.84	99.84	99.69
subj19	695	0	0	0	100	100	100
subj20	1083	0	0	0	100	100	100
overall	16,244	12	8	0.12	99.95	99.93	99.88

Table 3 Performance comparison of peak detection methods

Database (method)	TP	FP	FN	Se, %	Pp, %	OA, %
IITBBS (our method)	16,244	12	8	99.95	99.93	99.88
MIT-BIH SLP (our method)	87,314	99	28	99.97	99.89	99.85
MIT-BIH SLP [18]	67,055	264	70	99.89	99.59	99.49
CSL [15]	13,055	21	24	99.82	99.84	99.66
CSL [16]	12,979	110	100	99.24	98.48	98.41
—	—	—	—	—	—	—
CSL [17]	13,050	32	20	99.85	99.76	99.6
CSL (our method)	13,057	9	22	99.83	99.93	99.76

Table 4 Robustness of the ZFR-based peak detection method

Record	TP	FP	FN	Se (%)	Pp (%)	OA (%)
original	13,057	9	22	99.83	99.93	99.76
SNR = 30 dB	13,056	9	22	99.83	99.93	99.76
SNR = 25 dB	13,052	9	24	99.82	99.93	99.75
SNR = 20 dB	13,055	10	25	99.81	99.92	99.73
SNR = 15 dB	13,047	12	28	99.79	99.91	99.69
SNR = 10 dB	13,047	17	28	99.79	99.87	99.66
SNR = 5 dB	13,047	21	32	99.76	99.84	99.60

for noisy PPG signals with signal-to-noise ratio (SNR) values of 30, 25, 20, 15, 10 and 5 dB. In this study, we observed that the ZFR-based method results in more false positives due to the spurious spikes present in the ZFFS signal under low SNR conditions. Therefore, we implement the moving average to smooth out the spurious spikes in the portions of the zero-crossing points of the ZFFS signal. Results also show that the smoothing process reduces the peak-amplitudes for very low-amplitude PPG signals. Therefore, the method had more false negatives than false positives for very-small pulse amplitudes. However, the detection rates of the method demonstrate that the method is robust in detecting the peaks under noisy PPG signals with low SNR conditions. Evaluation results show that the ZFR-based method achieves an average Se of 99.76%, Pp of 99.84%, and OA of 99.60% for the PPG signals with SNR of 5 dB. By comparing the different signal processing techniques, it is noticed that the ZFR-based systolic peak detection method is simple as compared with the current state-of-the-art detection methods based on the wavelet transform, EMD, Hilbert transforms and filtering methods with multiple detection results.

4. Conclusion: This Letter presents a simple ZFR-based systolic peak detection method without using the search back mechanism to reject or include the noise or missed peaks. The method is evaluated using different kinds of PPG signals taken from the standard MIT-BIH-Polysomnographic and CSL databases and the real-time PPG signals recorded at our Biomedical System Lab. The method had an average Se of 99.95%, and Pp of 99.89% on the total number of 116,673 peaks. Results further show that the method had an average Se = 99.76%, Pp = 99.84% and OA = 99.60% for noisy PPG signals with a SNR of 5 dB. Evaluation results demonstrate the robustness of the ZFR-based method under severe noisy PPG signals. As compared with different signal processing stages of existing detection methods, the ZFR-based peak detection method is simple and reliable in achieving better detection rates under different kinds of PPG signal patterns and noises.

5. Funding and declaration of interest: This research work was supported in part by the Special Manpower Development Program for Chips to System Design (SMDP-C2SD) under Ministry Of Electronics & Information Technology (MeitY) Grant, Government of India (grant no. RP089). Conflict of interest: none declared.

6 References

[1] Jarchi D., Casson A.J.: 'Towards photoplethysmography based estimation of instantaneous heart rate during physical activity', *IEEE Trans. Biomed. Eng.*, 2017, **64**, (9), pp. 2042–2053
[2] Temko A.: 'Accurate wearable heart rate monitoring during physical exercises using PPG', *IEEE Trans. Biomed. Eng.*, 2017, **64**, (9), pp. 2016–2024
[3] Dao D., *ET AL.*: 'A robust motion artifact detection algorithm for accurate detection of heart rates from photoplethysmographic signals using time-frequency spectral features', *IEEE J. Biomed. Health Inf.*, 2017, **21**, (5), pp. 1242–1253
[4] He X., *ET AL.*: 'Secondary peak detection of PPG signal for continuous cuffless arterial blood pressure measurement', *IEEE Trans. Instrum. Meas.*, 2014, **63**, (6), pp. 1431–1439
[5] Aboy M., *ET AL.*: 'An automatic beat detection algorithm for pressure signals', *IEEE Trans. Biomed. Eng.*, 2005, **52**, (10), pp. 1662–1670
[6] Gil E., *ET AL.*: 'PTT variability for discrimination of sleep apnea related decreases in the amplitude fluctuations of PPG signal in children', *IEEE Trans. Biomed. Eng.*, 2010, **57**, pp. 1079–1088
[7] Ricardo Ferro B.T., *ET AL.*: 'Automated detection of the onset and systolic peak in the pulse wave using Hilbert transform', *Biomed. Signal Process. Control*, 2015, **20**, pp. 78–84
[8] Iliev I., *ET AL.*: 'Algorithm for real-time pulse wave detection dedicated to non-invasive pulse sensing'. Proc. IEEE Computing in Cardiology, September 2012, pp. 777–780
[9] Jang D.G., *ET AL.*: 'A robust method for pulse peak determination in a digital volume pulse with a wandering baseline', *IEEE Trans. Biomed. Circuits Syst.*, 2014, **8**, (5), pp. 729–737
[10] Jang D.G., *ET AL.*: 'A knowledge-based approach to arterial stiffness estimation using the digital volume pulse', *IEEE Trans. Biomed. Circuits Syst.*, 2012, **6**, (4), pp. 366–374
[11] Shin H.S., *ET AL.*: 'Adaptive threshold method for the peak detection of photoplethysmographic waveform', *Comput. Biol. Med.*, 2009, **39**, (12), pp. 1145–1152
[12] Chang K.M., Chang K.M.: 'Pulse rate derivation and its correlation with heart rate', *J. Med. Biol. Eng.*, 2009, **29**, (3), pp. 132–137
[13] Lee C.K., *ET AL.*: 'A study on comparison PPG variability with heart rate variability in the sitting position during paced respiration'. Proc. World Congress on Medical Physics and Biomedical Engineering, September 2010, pp. 1703–1705
[14] Lazaro J., *ET AL.*: 'Pulse rate variability analysis for discrimination of sleep-apnea-related decreases in the amplitude fluctuations of pulse photoplethysmographic signal in children', *IEEE J. Biomed. Health Inf.*, 2014, **18**, (1), pp. 240–246
[15] Li B.N., *ET AL.*: 'On an automatic delineator for arterial blood pressure waveforms', *Biomed. Signal Proc. Control*, 2010, **5**, (1), pp. 76–81
[16] Paradkar N., Chowdhury S.R.: 'Primary study for detection of arterial blood pressure waveform components'. Proc. 37th. Int. Conf. on IEEE EMBS, August 2015, pp. 1959–1962
[17] Ostojic V., *ET AL.*: 'Empirical mode decomposition based real-time blood pressure delineation and quality assessment'. Proc. IEEE Computing in Cardiology, September 2013, vol. 40, pp. 221–224
[18] Raju D.S., *ET AL.*: 'An automated method for detecting systolic peaks from arterial blood pressure signals'. Proc. Int. Conf. IEEE Students' Technology Symp. (TechSym), February 2014, pp. 41–46
[19] Yegnanarayana B., Murty K.S.R.: 'Event-based instantaneous fundamental frequency estimation from speech signals', *IEEE Trans. Audio, Speech Lang. Process.*, 2009, **17**, (4), pp. 614–625
[20] Deshpande P.S, Manikandan M.S.: 'Effective glottal instant detection and electroglottographic parameter extraction for automated voice pathology assessment', *IEEE J. Biomed. Health Inf.*, 2018, **22**, (2), pp. 398–408
[21] The MIT-BIH Polysomnographic Database. Available at https://physionet.org/physiobank/database/slpdb/
[22] Complex System Laboratory (CSL Benchmark Dataset): Available at https://www.pdx.edu/biomedical-signal-processing-lab/biomedical-detection-benchmarks
[23] Miniaturized Pulse Oximeter Reference Design: http://www.ti.com/lit/ug/tidu542/tidu542.pdf